

# Assessment of the Noise Reduction Potential of Advanced Subsonic Transport Concepts for NASA's Environmentally Responsible Aviation Project

Russell H. Thomas<sup>1</sup>, Casey L. Burley<sup>2</sup>, and Craig L. Nickol<sup>3</sup>  
NASA Langley Research Center, Hampton, VA 23681 USA

Aircraft system noise is predicted for a portfolio of NASA advanced concepts with 2025 entry-into-service technology assumptions. The subsonic transport concepts include tube-and-wing configurations with engines mounted under the wing, over the wing nacelle integration, and a double deck fuselage with engines at a mid-fuselage location. Also included are hybrid wing body aircraft with engines upstream of the fuselage trailing edge. Both advanced direct drive engines and geared turbofan engines are modeled. Recent acoustic experimental information was utilized in the prediction for several key technologies. The 301-passenger class hybrid wing body with geared ultra high bypass engines is assessed at 40.3 EPNLdB cumulative below the Stage 4 certification level. Other hybrid wing body and unconventional tube-and-wing configurations reach levels of 33 EPNLdB or more below the certification level. Many factors contribute to the system level result; however, the hybrid wing body in the 301-passenger class, as compared to a tube-and-wing with conventional engine under wing installation, has 11.9 EPNLdB of noise reduction due to replacing reflection with acoustic shielding of engine noise sources. Therefore, the propulsion airframe aeroacoustic interaction effects clearly differentiate the unconventional configurations that approach levels close to or exceed the 42 EPNLdB goal.

## Nomenclature

$AOA$	=	angle of attack
$EPNL$	=	effective perceived noise level, decibels (dB)
$f$	=	frequency (Hz)
$M_0$	=	free stream Mach number
$PNLT$	=	tone corrected perceived noise level, decibels
$P_{rms}^2$	=	mean square acoustic pressure
$S$	=	suppression function
$SPL$	=	sound pressure level, decibels
$\theta$	=	polar angle, degrees, with zero degrees in direction of flight
$\phi$	=	azimuthal angle, degrees, with zero degrees directly under flight path

## I. Introduction

NASA's Environmentally Responsible Aviation (ERA) Project has focused since inception in 2009 on developing and demonstrating technologies for integrated aircraft systems that could simultaneously meet aggressive goals for fuel burn, noise, and emissions. The fuel burn goal is for a reduction of 50% in block fuel relative to a best-in-class aircraft in 2005; the noise goal is 42 EPNLdB cumulative below the Federal Aviation Administration Stage 4 requirement; and the emissions goal is for a reduction of 75% in landing and takeoff NO<sub>x</sub> (oxides of nitrogen) levels below the CAEP 6 (Committee on Aviation Environmental Protection) standard. The target date is 2020 for key technologies to be at a technology

---

<sup>1</sup> Senior Research Engineer, Aeroacoustics Branch, MS 461, AIAA Senior Member

<sup>2</sup> Senior Research Engineer, Aeroacoustics Branch, MS 461, AIAA Senior Member

<sup>3</sup> Senior Aerospace Engineer, Aeronautical Systems Analysis Branch, MS 442, AIAA Senior Member

readiness level (TRL) of 4-6 (corresponding to a system or sub-system prototype demonstrated in a relevant environment). This timeline aligns with a projected aircraft entry-into-service of 2025. NASA defines these goals with this timeframe with the term N+2 reflecting aircraft technology that is two generations beyond that represented by the 2005 best-in-class baseline aircraft. The noise goal has been seen as a significant challenge, and through past research it has been thought that a configuration change would likely be necessary to enable the achievement of the 42 dB noise goal. Out of possible advanced aircraft concepts, past research (Refs 1-5) has shown the Hybrid Wing Body (HWB) configuration, together with advanced technologies, to be one of the most likely configurations to reach the noise goal.

Thomas et al. (Ref 2) gives a brief description of the early work at NASA leading to setting the N+2 noise goal at the 42 dB level. Thomas et al. (Ref 2) and Czech et al. (Ref 3) also describe the first major combined experimental (Boeing Low Speed Aeroacoustics Facility (LSAF)) and assessment effort to develop the technical roadmap to achieve the 42 dB goal on an HWB configuration, focusing only on the noise goal. Also as part of the combined research reported (Ref 2-3) is the experimental campaign to acquire experimental data used in the noise assessment of the HWB for the propulsion airframe aeroacoustic (PAA) interactions that were difficult to predict at that time. Also reported by Czech et al. (Ref 3) is the successful development of technology to increase the noise reduction obtained from shielding of the jet noise sources by a given dimension of the airframe. A subsequent experimental campaign was conducted on a Boeing HWB design, the N2A, that was designed to meet the 42 dB goal but with a 25% fuel burn reduction. Burley et al. (Ref 4) reported the noise assessment results of the N2A including extensive use of data from the N2A aeroacoustic test. Guo et al. (Ref 5) documents the noise assessment of a more advanced Boeing HWB concept designed to meet the ERA N+2 goals simultaneously and also compares the noise assessment processes used by NASA and used by Boeing for the HWBs that were being developed during the period of the first half (Phase 1) of ERA, from 2009 to 2012. These efforts (Refs 1-5) also chronicle, up to the first half of ERA, the development of the NASA noise assessment process for advanced and unconventional aircraft concepts such as the HWB.

In the final three years (Phase 2) of ERA, 2012-2015, annual aircraft level system noise assessments have been conducted by the ERA team on a portfolio of N+2 aircraft concepts to demonstrate by analysis the performance of the integrated advanced vehicles and technologies compared to the original ERA N+2 goals. The aircraft concepts include a full range of technology assumptions deemed feasible for entry-into-service in the 2025 timeframe. These concepts incorporate the results of a series of experiments performed throughout the six years of ERA and specifically by Integrated Technology Demonstration (ITD) efforts in the final three years of ERA that were conducted in collaboration with industry partners. Each annual assessment included increasingly refined aircraft models and new experimental inputs, which were available at the time of the assessment. Nickol and Haller (Ref 6) describes the modeling of the N+2 aircraft in detail and the resulting fuel burn and emissions reduction assessment results achieved at the conclusion of ERA in 2015.

The ERA N+2 aircraft have been designed with a balanced approach to simultaneously meet aggressive goals for reductions in the fuel burn, emissions, and noise. Design parameters, operational refinements, and noise reduction technology that have an impact on aircraft level noise have all been integral to the N+2 aircraft design process together with fuel burn and emissions reduction requirements. Technologies key to obtaining all three goals simultaneously have been the focus of the ERA ITD studies and, as a result, have produced higher TRL data relevant to the noise assessment. As a result, the noise assessment process developed for the ERA N+2 aircraft has been driven to a fidelity and rigor not typically associated with conceptual level system noise prediction. The many factors driving the ERA noise assessment include accurate assessment to reflect the high TRL of ERA; multiple aircraft configurations each with multiple impacts on noise; a range of advanced technology assumptions for the 2025 timeframe; high fidelity acoustic data generated from three of the ERA ITD studies as well as several other earlier large experimental campaigns and finally, the aggressive noise goal that is difficult to achieve itself and especially when including tradeoffs in design to also achieve the other goals.

The purpose of this paper is to describe the noise assessment prediction method developed for the ERA N+2 aircraft and report the cumulative aircraft system level results achieved at the conclusion of ERA in 2015. This paper also will provide insight into the impact of key technologies, design parameters, and operational characteristics relative to the cumulative noise results achieved.

## II. Advanced N+2 Aircraft Concept Description

Eight ITD research efforts were completed in the second half of ERA and have influenced the design and assessment results of the N+2 aircraft concepts. The reader is referred to the publications from the ITD teams for details on those research efforts. Nickol and Haller (Ref 6) summarize the eight ITDs and the ITD results that were utilized to form the technology assumptions for the aircraft system level modeling of the N+2 vehicles. The eight ITDs are listed here simply for completeness, and the titles are self-descriptive of the technologies that are the subjects of the ITDs:

- ITD 12A+ Active Flow Control (AFC) Enhanced Vertical Tail plus Advanced Wing Flight Experiment with Insect Accretion Mitigation (IAM) and Natural Laminar Flow (NLF) features
- ITD 21A Damage Arresting Composites Demonstration
- ITD 21C Adaptive Compliant Trailing Edge (ACTE) Flight Experiment
- ITD 30A Highly Loaded Front Block Compressor
- ITD 35A 2<sup>nd</sup> Generation Geared Turbofan Propulsor
- ITD 40 Low NO<sub>x</sub> Fuel Flexible Combustor
- ITD 50A Flap Edge and Landing Gear Noise Reduction
- ITD 51A Ultra-High-Bypass (UHB) Ratio Engine Integration for Hybrid Wing Body Concepts.

All ITDs developed technologies that impacted the aircraft system level modeling of the ERA N+2 vehicles. Several ITD technologies impact N+2 aircraft noise indirectly, for example light weight structure enabled by ITD21A technology. Those ITD results that impact noise more directly or are used directly in the noise assessment will be discussed in more detail below.

Nickol and Haller (Ref 6) provides additional details of the modeling and the technology assumptions used in developing the ERA N+2 vehicle portfolio of thirteen aircraft concepts. This section will only describe the vehicles, design parameters, and performance results that impact directly the noise assessment results to follow. The noise assessment results will also include the aircraft takeoff and landing performance modeled by Nickol and Haller (Ref 6) for the sideline (also known as lateral), cutback (also known as flyover), and approach noise certification conditions.

In addition to modeling 2025 entry-into-service technology, another key aspect of the ERA N+2 aircraft is the inclusion of four aircraft configurations. The tube-and-wing (T+W) configuration with engines mounted underneath the wing, representing the most common configuration of current subsonic transports, is included in the N+2 portfolio with all the applicable N+2 technology assumptions. Using the same N+2 technology assumptions, the T+W configurations provide a basis to determine the potential additional benefits possible with the more unconventional configurations.

An unconventional T+W with the engines integrated with the top of the wing is referred to as the Over-Wing-Nacelle (OWN) configuration and has been investigated by NASA (Ref 7). Additional features of the OWN are an unswept wing between the nacelle and the fuselage as well as shaping to minimize the shocks in this region at transonic cruise conditions. Another unconventional tube-and-wing configuration is distinguished with a double deck fuselage and the engine mounted from the fuselage and positioned at the mid-fuselage location so that the inlet of the nacelle is over the trailing edge of the main wing. This is termed the mid-fuselage nacelle (MFN) configuration and is a NASA version of a concept reported by Boeing (Ref 8) with a subsequent assessment by Guo et al. (Ref 9). From an aircraft noise perspective, both the OWN and MFN, while still fundamentally T+W configurations, do represent the potential for lower noise over the traditional engine-under-wing T+W by introducing a significant noise shielding advantage. The OWN can shield the aft radiated engine noise but can also introduce a jet scrubbing noise source, and the MFN can shield the inlet radiated fan noise and could further enable, therefore, short inlets for UHB engines. It should be noted that the OWN could be scaled to include smaller seat classes than the MFN, which is only practical for mid range, and larger seat classes due to the double deck. On the other hand, the double deck arrangement results in a total of three aisles, and if integrated properly with a two level jet way, the MFN could enable expedited passenger loading times over the equivalent single deck configuration. It can be seen that both the OWN and the MFN introduce additional tradeoffs that require a more thorough investigation. In this paper, only the system noise of the concepts will be assessed.

The fourth configuration in the N+2 portfolio is the hybrid wing body (HWB) configuration that has been researched by both Boeing and NASA for many years (Ref 1-5, 8, 10-15). The earlier version of the HWB (Ref 10) configured the engines at the trailing edge of the aircraft with the engine nozzle exit plane downstream of the trailing edge. As the potential of the HWB to achieve the N+2 noise goal was being

developed (Ref 1) the later versions position the engines so that the engine core nozzle exit plane is upstream of the airframe trailing edge. This has been a significant design change with implications for propulsion airframe integration at cruise conditions and for low speed operability (and the subject of ITD51A, Ref 16); however, it has also enabled the HWB to shield both forward and aft-radiated engine noise.

Engine architecture is another major technology to consider for the 2025 timeframe. In general, compared to today’s engines, the N+2 engines follow the trends toward larger diameters, lower fan pressure ratios and higher pressure ratio cores enabled by incorporating advanced materials and shorter inlets. The NASA Glenn Research Center (GRC) Propulsion System Analysis Branch has modeled both ultra high bypass ratio Direct Drive (DD) and Geared Turbofan (GTF) engines for the requirements and thrust classes of the ERA N+2 portfolio and using GRC’s standard tools and processes including NPSS (Numerical Propulsion System Simulation, Ref 17) and WATE++ (Weight Analysis of Gas Turbine Engines, Ref 18). In keeping with the overall study objectives, these engines are balanced designs to best meet all three goals simultaneously. In addition to the engine cycle trends mentioned above, another important impact of the N+2 airframe technology is that the thrust requirements are significantly lower compared to a current aircraft in the same class. This is due to the impact of the airframe technologies that have reduced weight and drag considerably and therefore thrust. In addition to the impact of the engine cycle, several key engine parameters, design features and tradeoffs will be listed and discussed in the noise assessment results section.





Five vehicle sizes (passenger classes) are examined. In each of five passenger classes, the N+2 airframes are matched as appropriate with the proper thrust class engine of either DD or GTF type. The thirteen vehicles are sized using the NASA FLOPS (Flight Optimization System) code and the high lift performance is modeled with a modified vortex lattice method (MVL) (Ref 6). Table 1 shows the five aircraft classes in the ERA N+2 portfolio by number of passengers and the configurations that are included. Tables 2-5 list the thirteen vehicles and some of the key overall performance parameters and sizing information including the takeoff gross weight (TOGW) and operating empty weight (OEW). Table 2 has both the Regional (98 passengers) and the Single Aisle (160 passengers) class vehicles. Table 3 has both the Small Twin Aisle (216 passengers) and the Very Large Twin Aisle (400 passengers) class vehicles. Table 4 has the Large Twin Aisle (301 passengers) class vehicles. Table 5 lists the final aircraft, the MFN301, which is also in the 301-passenger class. Each class has a NASA model of a reference aircraft to represent current, in service, aircraft performance as a baseline. Again, the reader is referred to Nickol and Haller (Ref 6) for more description of the engine and aircraft modeling and more detailed specifications for the performance and sizing of each of the aircraft including the reference aircraft. Tables 2-5 also show some of the key parameters and specifications that are relevant for the noise assessment. For example the acoustic liner length in the inlet is non-dimensionalized by the fan diameter (D) and the aft bypass duct liner length is non-dimensionalized by the effective height of the aft duct (H).

**Table 1. Aircraft concepts and nomenclature of the ERA N+2 study (from Nickol and Haller Ref 6).**


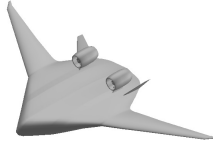
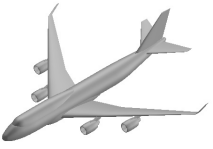
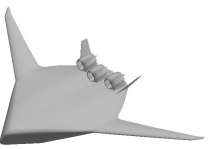
Vehicle Class	Abbreviation	Number of Passengers	N+2 T+W Nomenclature	Unconventional	Abbreviation
Regional Jet	RJ	98	T+W98	Over-Wing-Nacelle	OWN98
Single Aisle	SA	160	T+W160	Over-Wing-Nacelle	OWN160
Small Twin Aisle	STA	216	T+W216	Hybrid-Wing-Body	HWB216
Large Twin Aisle	LTA	301	T+W301	Hybrid-Wing-Body	HWB301
				Mid-Fuselage Nacelle	MFN301
Very Large Twin Aisle	VLTA	400	T+W400	Hybrid-Wing-Body	HWB400

An output from the aircraft modeling was the low speed flight path, as well as aircraft and engine parameters as a function of the flight path corresponding to the three aircraft noise certification points of sideline/lateral, flyover with cutback, and approach. Tables 2-5 also show lift-to-drag, bypass ratio (BPR), and fan pressure ratio (FPR), three key parameters, at each of the three certification points to provide a comparison between the vehicles, as well as an indication of how much the key parameters change between the three certification points.



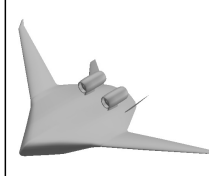
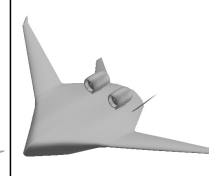
**Table 2. Vehicle Models for the N+2 Regional Jet and Single Aisle Class T+W and OWN.**

		Regional Jet		Single Aisle	
					
	Units	T+W98-DD	OWN98-DD	T+W160-GTF	OWN160-GTF
TOGW	lb	90,858	89,790	146,251	141,868
OEW	lb	53,631	52,861	81,688	78,377
Payload	lb	21,605	21,605	37,760	37,760
Total Fuel	lb	15,623	15,324	26,803	25,731
Wing Span	ft	97.0	96.9	114	112.2
Takeoff Field Length	ft	6,085	5,948	7,386	6,567
Main Gear Type		2 wheel G550-like	2 wheel G550-like	2 wheel 737-like	2 wheel 737-like
Main Gear Strut Length	ft	7.3	6	10.4	6.6
Thrust per Engine	lb	15,000	15,000	21,500	21,600
Fan Diameter	in	55.2	55.2	83.9	84.1
Fan Rotor/Vane Count		18/48	18/48	18/40	18/40
Inlet Liner Length/D		0.34	0.34	0.34	0.34
Aft Duct Liner Length/H		4.48	4.48	1.83	1.83
<b>Parameters at Noise Certification Points</b>					
Takeoff:					
	Lift/Drag	12.52	12.52	14.6	14.4
	Bypass Ratio	10.01	10.01	25.48	25.56
	Fan Pressure Ratio	1.51	1.51	1.23	1.23
Cutback:					
	Lift/Drag	12.01	12.01	14.46	14.06
	Bypass Ratio	10.01	10.03	28.26	28.42
	Fan Pressure Ratio	1.38	1.37	1.16	1.16
Approach:					
	Lift/Drag	8.87	8.86	9.46	9.41
	Bypass Ratio	12.55	12.55	33.35	33.41
	Fan Pressure Ratio	1.12	1.12	1.06	1.06


**Table 3. Vehicle Models for the N+2 Small Twin Aisle and Very Large Twin Aisle Class T+W and HWB.**

		Small Twin Aisle		Very Large Twin Aisle	
					
	Units	T+W216-GTF	HWB216-GTF	T+W400-GTF	HWB400-GTF
TOGW	lb	286,926	313,859	686,046	702,527
OEW	lb	153,101	181,152	358,126	385,353
Payload	lb	44,500	44,500	147,840	147,840
Total Fuel	lb	89,325	88,206	180,079	169,334
Wing Span	ft	180.9	220	247.1	260
Takeoff Field Length	ft	8,990	5,821	10,468	10,491
Main Gear Type		4 wheel 767-like	4 wheel 767-like	total of 4, each 4 wheel 767-like	6 wheel 777-like
Main Gear Strut Length	ft	15	6.6	10.6 on fuselage, 21.2 on wing	8.4
Thrust per Engine	lb	45,327	45,566	44,707	54,648
Fan Diameter	in	115.7	116.1	115	119.1
Fan Rotor/Vane Count		18/40	18/40	18/40	16/36
Inlet Liner Length/D		0.34	0.34	0.34	0.33
Aft Duct Liner Length/H		1.99	1.99	1.99	2.13
<b>Parameters at Noise Certification Points</b>					
Takeoff:					
	Lift/Drag	11.91	24.7	9.97	22.7
	Bypass Ratio	22.98	23.17	22.99	18.74
	Fan Pressure Ratio	1.25	1.25	1.25	1.3
Cutback:					
	Lift/Drag	11.8	23.6	9.93	22.06
	Bypass Ratio	25.16	28.36	25.62	22.96
	Fan Pressure Ratio	1.2	1.12	1.19	1.16
Approach:					
	Lift/Drag	8.51	11.04	9.37	12.01
	Bypass Ratio	31.97	32.74	31.88	27.77
	Fan Pressure Ratio	1.06	1.04	1.06	1.05

**Table 4. Vehicle Models for the N+2 Large Twin Aisle Class T+W and HWB.**

					
	Units	<b>T+W301-DD</b>	<b>T+W301-GTF</b>	<b>HWB301-DD</b>	<b>HWB301-GTF</b>
TOGW	lb	570,195	570,533	537,641	534,491
OEW	lb	265,290	270,084	251,281	253,326
Payload	lb	118,100	118,100	118,100	118,100
Total Fuel	lb	186,805	182,349	168,259	163,065
Wing Span	ft	226.5	226.6	250	250
Takeoff Field Length	ft	9,231	9,019	9,171	8,541
Main Gear Type		6 wheel 777-like	6 wheel 777-like	6 wheel 777-like	6 wheel 777-like
Main Gear Strut Length	ft	17.1	19.2	7.4	7.4
Thrust per Engine	lb	71,800	74,000	65,989	69,398
Fan Diameter	in	130.6	151.3	118.7	132.4
Fan Rotor/Vane Count		16/42	16/36	16/42	16/36
Inlet Liner Length/D		0.33	0.33	0.33	0.33
Aft Duct Liner Length/H		2.96	1.57	3.33	1.99
<b>Parameters at Noise Certification Points</b>					
Takeoff:					
Lift/Drag		14.44	14.47	23.98	24.1
Bypass Ratio		16.55	23.28	13.74	18.74
Fan Pressure Ratio		1.37	1.25	1.42	1.3
Cutback:					
Lift/Drag		14.2	14.19	23.17	23.2
Bypass Ratio		17.91	25.14	16.61	22.96
Fan Pressure Ratio		1.29	1.2	1.23	1.16
Approach:					
Lift/Drag		8.94	8.95	11.04	11.04
Bypass Ratio		21.99	32.21	19.17	27.81
Fan Pressure Ratio		1.08	1.06	1.07	1.05

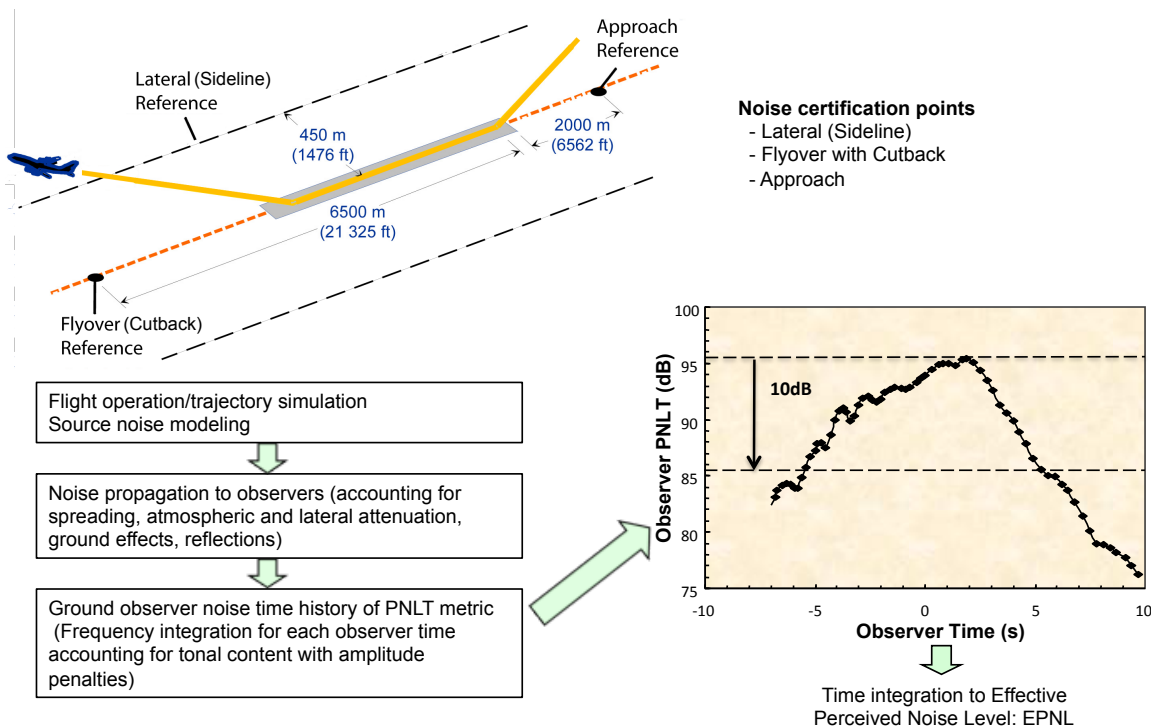
**Table 5. Vehicle Model for the N+2 Large Twin Aisle Class MFN.**

		<b>Large Twin Aisle</b>	
			
	Units	<b>MFN301-GTF</b>	
TOGW	lb	540,837	
OEW	lb	259,943	
Payload	lb	118,100	
Total Fuel	lb	162,795	
Wing Span	ft	207.7	
Takeoff Field Length	ft	7,359	
Main Gear Type		6 wheel 777-like	
Main Gear Strut Length	ft	9.6	
Thrust per Engine	lb	65,500	
Fan Diameter	in	149.2	
Fan Rotor/Vane Count		16/36	
Inlet Liner Length/D		0.33	
Aft Duct Liner Length/H		1.57	
<b>Parameters at Noise Certification Points</b>			
Takeoff:			
Lift/Drag		13.92	
Bypass Ratio		23.34	
Fan Pressure Ratio		1.25	
Cutback:			
Lift/Drag		13.5	
Bypass Ratio		25.38	
Fan Pressure Ratio		1.2	
Approach:			
Lift/Drag		8.9	
Bypass Ratio		31.91	
Fan Pressure Ratio		1.06	

### III. Noise Assessment Process

The ERA noise assessment process uses a similar approach for predicting the noise of advanced and unconventional aircraft as was taken in the first assessment that assessed an HWB concept relative to the 42 dB goal at the beginning of ERA (Ref 2). The ERA noise assessment process includes utilizing the best noise assessment practices, databases, and methods developed at NASA over the previous decades for predicting community noise. In addition, during the second half of ERA, the noise assessment process has been continuously improved through increasingly detailed aircraft definition, component modeling improvements, incorporation of the latest information from the ITD experiments, as well as through key experiments from the first Phase of ERA, and through improved vehicle design and flight path iterations with the aircraft modeling and propulsion teams. This section will describe the cumulative noise metric calculated, the overall ERA noise assessment process as developed during the second Phase of ERA and include a description of the modeling of selected technologies and aircraft noise effects. For several technologies and integration effects, the prediction is linked to the technology and the available data and information.

An overview chart for the cumulative noise metric is shown in Figure 1. Specifically, the noise metric for the 2025 aircraft models is certification community noise as defined in the Code of Federal Regulations (CFR) Title 14, Part 36. In order to obtain Federal Aviation Administration (FAA) certification, the noise of an aircraft must be measured according to the rules of Part 36. In the context of the research and technology maturation of integrated aircraft systems, the noise of ERA aircraft concept models is predicted according to the same Part 36 rules. Part 36 defines specific parameters for aircraft noise at each of three certification points.



**Figure 1. Noise certification flight paths and metric definitions used in the system noise assessment process. (Definitions guided by the Code of Federal Regulations (CFR) Title 14 Part 36)**

Takeoff noise with the aircraft at full power is predicted along a line offset and parallel to the runway and flight path by 1476 feet. Maximum noise along this parallel line is the lateral (also known as sideline) certification noise point and occurs typically for conventional aircraft when the aircraft has reached an altitude of 1000 ft. As part of a ground rule meant to establish both an equal basis (for conventional and unconventional aircraft) and to standardize with industry practice, the ERA aircraft sideline noise is

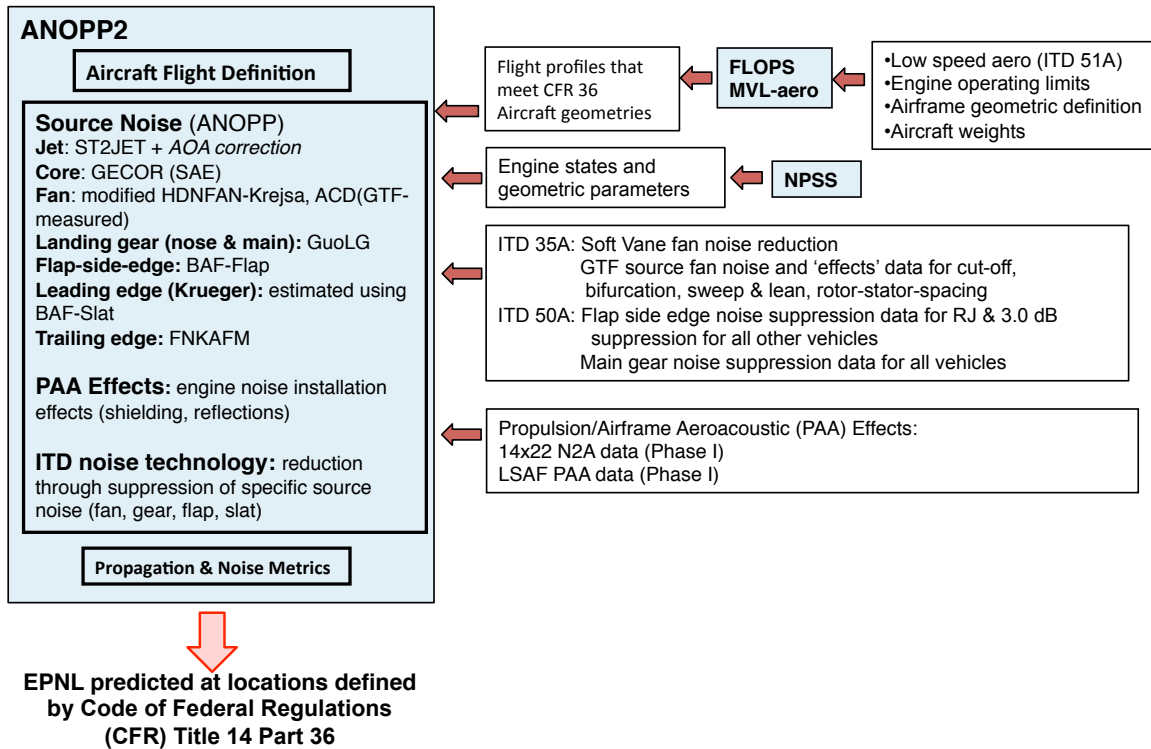
predicted also when the aircraft has reached an altitude of 1000 feet. The noise for the reduced power segment of the takeoff trajectory is obtained at the flyover or simply referred to as the cutback point. The cutback point is located directly under the flight path at a position that is 21,325 feet from brake release as shown in Figure 1. The aircraft is allowed to cutback on engine power but must maintain a climb gradient. The altitude of the aircraft at cutback and the engine throttle setting depend primarily on the aircraft's high lift and engine characteristics, both of which can impact the cutback noise level significantly. The third certification point, approach, characterizes the noise of the aircraft in the descent and landing configuration. On the approach trajectory, the aircraft must maintain a 3-degree glide slope. The approach point is measured when the aircraft is at 6562 feet from the end of the runway with engine power sufficient to abort landing and go-around with an eight second engine spool up. Separate computations are performed to obtain each of the approach, lateral, and flyover EPNL noise levels. This procedure is consistent with previous assessments performed by NASA (Ref 2) and Boeing (Ref 5).

At each of the three certification points, the Effective Perceived Noise Level (EPNL) in decibels is predicted for the aircraft. The EPNL is a mathematical formulation that provides a single number characterizing the relevant acoustical effects impacting human perception and annoyance. The EPNL at a certification point includes the integration over time of the tone corrected perceived noise level (PNLT), see Figure 1. The tone correction was developed to capture the additional impact of tones on human annoyance. The corrections are noise level penalties assigned based on the tone level and number of tones. The integration over time begins at a point 10 dB (in PNLT) below the peak value of PNLT and continues to the point in time when the aircraft PNLT is again 10 dB below the peak as the aircraft recedes from the certification point. Spherical spreading, atmospheric attenuation, and ground effects are accounted for in the propagation of the aircraft noise to the certification point.

After calculation of the EPNLdB at each of the three certification points, the cumulative noise is the simple addition of the EPNL of the three points. Furthermore, the cumulative noise is referenced relative to the certification level required by the FAA in Part 36; the current regulation is termed Stage 4 and is a function of aircraft weight and the number of engines. In sum, the cumulative noise (CUM) below Stage 4 is the final noise metric reported by ERA.

Figure 2 schematically shows the overall ERA noise assessment process. The noise assessment calculation is performed using NASA's multi-fidelity aeroacoustic framework known as the second generation Aircraft Noise Prediction Program (ANOPP2) (Ref 19). The ANOPP2 framework allows a user to develop acoustic analyses and couple results from these analyses with prediction methods and other data into a unified process. For ERA, analysis capabilities were developed to apply flight effects to the input measured source noise (which includes installation effects), combine those measurements with legacy ANOPP predictions of other sources, propagate to the far field, and compute noise metrics. In order to provide the best prediction of each engine and airframe component together with the propulsion airframe aeroacoustic (PAA) interaction effects, the best of measured data or existing prediction processes are used.





**Figure 2. Overall ERA Noise Assessment Process.**

The process requires the input of the complete aircraft including engine, airframe, and its flight path (Ref 6). The flight path definition must provide engine thrust, aircraft configuration, angle of attack, altitude, and velocity along the flight trajectory. In addition the engine state must also be provided along the flight path in order to define the parameters necessary for the prediction of each engine noise component. The airframe component geometric specifications are, in general, not typically necessary for the prediction of aircraft fuel burn reduction at the conceptual level; however, they are required for the noise prediction of the landing gear, flap, slat or Krueger flap airframe noise components. Tables 2-5 include a few of the key specifications that are indicative of design features that have a strong influence on noise and a few of the detailed airframe specifications necessary. The landing gear type is included in Tables 2-5 to reflect the complexity of the gear, which is a requirement for the landing gear noise prediction.

It is important to note that all of the ITD results are used in developing the technology assumptions that are utilized in defining the engines and airframes of the ERA aircraft models. In this way, there is an ERA technology impact inherent to the noise prediction even if no acoustic data from an ITD is used directly. This is most notably the case with the structural weight technology assumptions that result in a lighter weight aircraft compared to the baseline. Lighter weight structures together with reduced drag results in lower engine thrust and among other impacts can result in lower noise levels inherently but may not necessarily reduce noise relative to the Stage 4 level because that level is also a function of weight.

With the definition of the flight path, airframe, and engine components, the noise prediction of the components and interactions can proceed. The results of three ITDs directly provide information and data to the process as is shown in the right side of Figure 2. In addition, large wind tunnel studies during the first half of ERA were extensively used for PAA effects. The modeling of each noise source, noise reduction technology or interaction will be discussed separately.

### **A. Fan Noise**

Van Zante and Suder (Ref 20) describe an overview of the research of ITD35A, a research effort that provided fan source noise experimental data for a wind tunnel turbine powered fan noise simulator model of the Geared Turbofan (GTF) engine concepts, a design space for which there is yet no direct validated system noise prediction method available. The combination of GTF experimental fan noise data is

processed to provide a data-to-prediction method that can account for model scale to full scale, engine state, and thrust. The flow chart of the fan noise prediction process developed in part using the ANOPP2 framework is detailed in Figure 3. Additionally, the process in Figure 3 includes four more semi-empirical methods that have been developed in order to provide a more complete prediction of realistic effects with significant impact including:

- stator sweep and lean,
- rotor/vane ratio cut-off effect,
- rotor/stator spacing, and
- bifurcation.

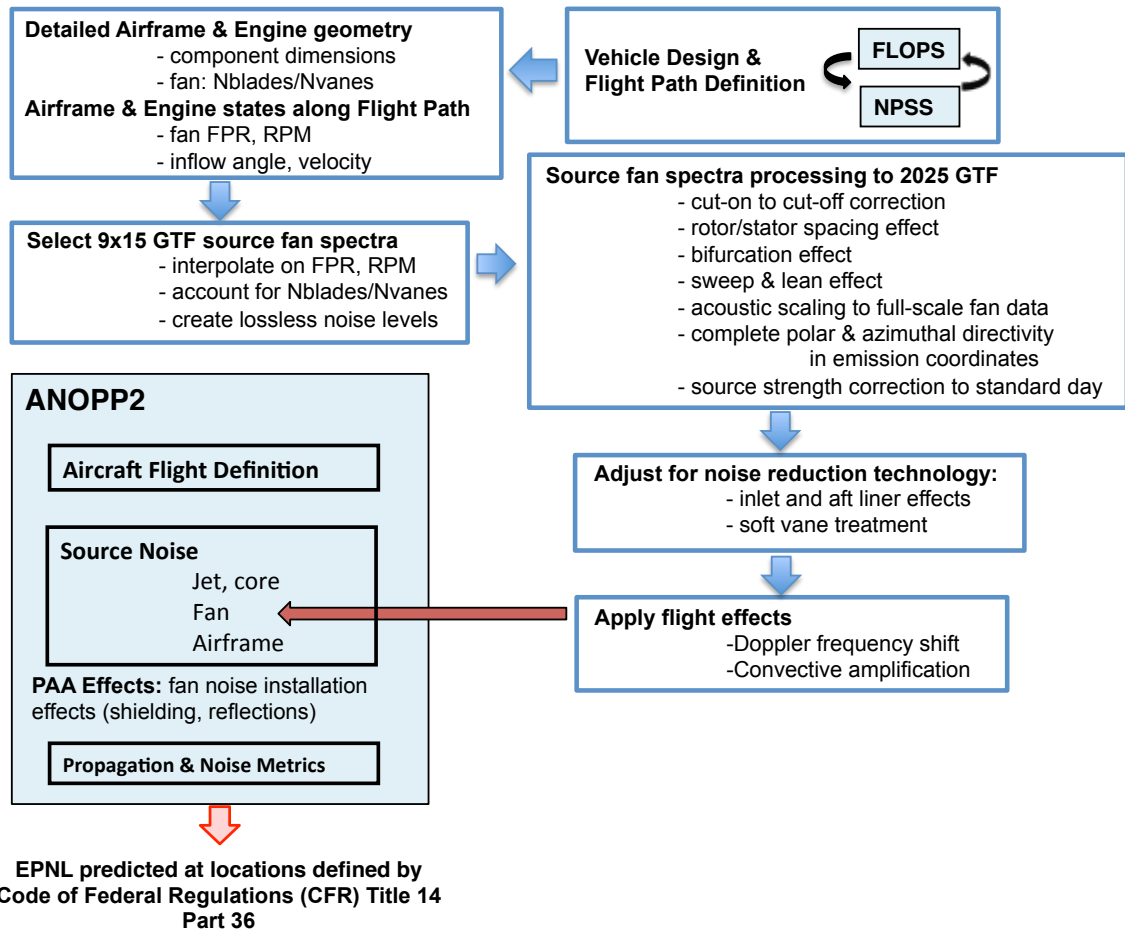


Figure 3. GTF fan noise processing steps (starting from measured GTF fan noise from ITD35A) within the overall ERA noise assessment process.

For the direct drive architecture of engines in the ERA portfolio, the existing Kresja (Ref 21) fan noise model (an option within the ANOPP-HDNFAN (Heidmann) fan module) is used, although with modifications in order to best account for the design space of the ERA direct drive engines. These modifications include a spectral amplitude adjustment of 2 dB and the application of the semi-empirical models (from the GTF sub-process) for rotor-stator spacing and bifurcation effect. The 2 dB increase of the spectral amplitude of the DD fan noise is based on a careful analysis of the Kresja prediction for a set of data (Ref 22) that is in a design space similar to the ERA DD fan. For the frequencies that correspond to the frequencies of the full-scale DD fan the Kresja prediction was found to be consistently 2 dB low.

## B. Core and Jet

Existing ANOPP modules for the prediction of core source noise, GECOR (Ref 23), and jet source noise, ST2JET (Ref 24), are used in the current study. While these methods have been used extensively in

prior NASA studies, they are older methods and, as all semi-empirical methods, have some limitations based on the original data from which the methods were developed and/or calibrated to. As with the other methods in this study, predictions are crosschecked with new information and databases from ERA or other recent research.

For the design parameters of the N+2 engine high pressure cores, the GECOR method is estimated to be consistently over predicting core noise. This is based on the combined experience of the systematic NASA assessment of the core noise prediction methods (Ref 22) and the evaluation of information obtained during ERA through ITD35A and ITD51A. As a result, a uniform 6 dB reduction at the spectral level is implemented. Core noise includes the noise of the combustor, compressor, and turbine.

The ST2JET method prediction of jet source noise was evaluated for use with the high bypass ratio jet parameters of the N+2 engines. Michael Doty compared predictions with experimental data of a bypass ratio 15 jet noise experiment obtained as part of a series of a PAA interaction tests in the Boeing Low Speed Aeroacoustic Facility (LSAF) (Ref 25). While there is variability with directivity angle, the ST2JET in general predicts reasonably well for the high bypass ratio jets. In addition, the prediction of jet noise component EPNL for the N+2 engines was also compared with information obtained through ITD51A and found to be reasonable.

In addition to jet source noise, a new correction for the jet source noise change due to angle of attack was developed by Doty based on measurements obtained as part of studies described in Refs 3, 25, and 26. The angle of attack introduces a cross flow to the jet at an angle equal to the angle of attack as modified by the installation effect of a wing and pylon. The cross flow changes the shear layer development and the trajectory of the secondary and the primary streams. Both the azimuthal and axial distributions of jet noise sources are modified. An empirical method to compute the increased noise level for jets at an angle of attack is available in SAE ARP876 for low BPR jets (BPR<5) and was further investigated by Mead and Kenning (Ref 27). To best fit the high bypass jet data, Doty developed a modified equation as follows:

$$\Delta dB = 0.5 * AOA * M_0 \left[ \frac{2.8\theta}{180} - 0.6 \right]^2$$

where AOA is the angle of attack in degrees,  $M_0$  is the flight Mach number and  $\theta$  is the polar directivity angle in degrees.

### C. Acoustic Duct Liner and Soft Vane

Conventional acoustic duct liner technology applied in the inlet, the interstage (between the fan rotor and the stator), and in the aft bypass duct is typically either of the single or double degree of freedom type. A single degree of freedom (SDOF) liner will have one layer of chambers of a depth nominally equal to one-quarter of the wavelength of the frequency targeted for peak attenuation. Typically, the first or second blade passage frequency tone is targeted; whichever provides the maximum impact on system level noise reduction. A double degree of freedom (DDOF) liner has two layers of chambers, separated by a porous septum, with each layer tuned to a different frequency.

The ANOPP-TREAT module provides a duct acoustic liner suppression method developed by Kontos et al. (Ref 28). The prediction method was developed based on an engine noise test database. The engines in the database are representative of commercial transport engines circa 1990 with DDOF liners in the inlet and SDOF acoustic liners in the bypass duct. Based on this database the liner suppression model predicts attenuation for both the inlet and the aft ducts based on the liner type, the effective length of the liner treatment and the effective aft duct height or inlet diameter. The liner suppression predicted by TREAT represents a prediction of the full-scale, full-fidelity impact of the SDOF of DDOF liner technology for the engines comprising the database. It should be noted that the liners in this database were targeted to the frequencies appropriate for the engines of the database, frequencies that may not be the same targets for an advanced concept engine.

Prior NASA advanced concept studies have included the predicted noise reduction from conventional liner technology with the addition of important effects. Thomas et al. (Ref 2) included duct liner noise reduction for the GE90-like engine on the HWB using the TREAT model, a process where the total engine noise was also calibrated to certification data. In addition to the conventional GE90-like acoustic liner, this study also included the estimate of the impact of a potential advanced concept duct liner, beyond SDOF and DDOF, and the application of duct liner to the upper bifurcator for increased treatment area.

Berton et al. (Ref 29) included the impact of DDOF liners by using a suppression map (noise reduction as a function of frequency and polar angle) based on data from a 22-inch diameter fan test. Berton et al. (Ref 29) also included the impact of two more unconventional liner technologies, soft vane and over-the-rotor. Soft vane technology is a single layer liner integrated into the stator vane of the fan to attenuate the fan-stator interaction noise at the source (Ref 30). Over-the-rotor is a metal bulk type liner treatment located in the fan casing immediately over the fan blade tip where the fan rub strip would typically be located (Ref 30). Berton et al. (Ref 29) included a 4 dB noise reduction, uniform over all angles and frequencies, from the combination of the soft vane and the over-the-rotor.

For the current study, the acoustic duct liner technology included in the N+2 aircraft and the prediction of the impact (Figure 3) adds the latest information and technology developments during the ERA project. Tables 2-5 list the available treatment lengths for the inlet and the aft duct for each aircraft engine. An interstage acoustic liner is added with an effective length to height ratio of 0.25 for all engines. As a good prediction of the impact at a full engine level, the TREAT model is used to predict the impact of conventional acoustic liner technology. To account for the spliceless manufacturing technology that has been introduced in recent years (as compared to the liners with splices of the TREAT database), the effective treatment length in the inlet, the interstage, and in the aft duct were each increased by 10% in a similar manner to Berton et al. (Ref 29). This factor is meant to account for the area increased by removing the splices and the reduction in tones brought about by removing the scattering effect of splices. Finally for the N+2 duct liner, the TREAT prediction is modified to reflect the impact of a multi-degree of freedom liner technology.

In recent years, NASA has developed a Multi-Degree of Freedom (MDOF) duct liner technology as described by Jones et al. (Ref 31). This technology features variable depth chambers uniformly distributed throughout the liner treatment area. The variable depth has the effect of broadening the tuning of the liner to include a wider frequency band as compared to either a single degree or a double degree of freedom liner. In this way the liner can have equivalent peak attenuation as a tuned double degree of freedom liner and with a wider frequency band, typically spanning at least the first and second blade passage frequency tones. The MDOF technology has been developed to include a recent TRL 5 test, sponsored by the NASA Advanced Air Transport Technology Project. Because of the TRL, this test is applicable to the N+2 timeframe. Considering these recent test results and projecting maturation to the N+2 timeframe, the predicted peak attenuation of the MDOF liner is set at just 5% more, in decibels, than the predicted peak attenuation from the TREAT model that reflects SDOF and DDOF design and manufacturing liner technology from circa 1990. In this way, the demonstrated advancements of the MDOF technology are included in the N+2 predictions while the levels are still considered reasonably conservative.

While considered a promising technology that is still under active development, the over-the-rotor liner technology TRL did not advance sufficiently during ERA and, therefore, it is not included in this N+2 assessment. The soft vane technology has demonstrated sufficient applicability and performance and is, therefore, included on all engines. The predicted soft vane noise suppression impact is developed from data obtained in a recent 1.3 pressure ratio 22-inch diameter fan noise test in the NASA Glenn 9x15 Low Speed Wind Tunnel and provided by Edmane Enviva. The noise reduction difference, hard wall stator to soft vane stator, is a function of polar angle and frequency and ranges from as much as 5 dB at the highest frequency to small increases at low frequencies. Several factors are considered in developing the N+2 soft vane suppression map (noise reduction as a function of frequency and polar angle) from the test data. First, the design of the soft vane for the 22-inch diameter fan test was developed with only an initial estimation of the target impedance. Second, model scale fabrication of a liner on a stator of a 22-inch fan introduces compromises that would not be present on the full-scale application. Therefore, considering the potential to design the soft vane to a specific full scale, N+2 fan and stator combination, a uniform 0.5 dB noise reduction is implemented at low frequencies of the model scale spectra and is considered appropriate for the N+2 timeframe of this study. The soft vane technology impact is then scaled and applied to the predicted fan source at the narrowband spectral level. Implementation at the narrowband source spectral level preserves the correct impact on fan tones and broadband noise.

The impact at the aircraft level of the soft vane technology and of the MDOF liner (compared to conventional duct liner) will be shown in the results section. Acoustic liner treatment to the upper and lower bifurcators could be added in a future iteration of this study.

#### **D. Airframe Noise Sources**

The airframe noise sources to be modeled include the nose and main landing gear, high lift trailing edge flap, leading edge Krueger flap, and trailing edge noise. The HWB aircraft do not have a high lift trailing edge flap; therefore, this source is not modeled for the HWB. The HWB does have trailing edge control elevons for directional stability control as well as positive pitching moment for takeoff. These control elevons and the side edges in particular have not been shown to be a significant noise source (Ref 4) and are not considered in this study.

The BAF (Landing Gear) (Ref 32) prediction method used in previous studies is replaced in this study with the newly developed GuoLG (Ref 33) method for both main and nose landing gear on all N+2 aircraft. Among other improvements described by Guo et al. (Ref 33), the GuoLG method includes effect of reflection of the landing gear source noise from the fuselage and landing gear doors. The fuselage planform, leading edge and trailing edge device deflections, and angle of attack are all modeled, and the reflection is predicted by a ray acoustics method. The resulting detailed directivity of landing gear noise including reflections provides a high fidelity noise prediction that has been validated with a range of wind tunnel and flight test data (Ref 33). The BAF (Flap) (Ref 34) is used for the noise from trailing edge high lift flaps on all the N+2 T+W, OWN, and MFN aircraft. The BAF (Slat) (Ref 35) method is used to estimate the noise from leading edge Krueger flaps that are configured on all the N+2 aircraft. The specifications of the Krueger flap on the N+2 aircraft are inputs to the BAF (Slat) method. Due to the expected differences in acoustic sources between a conventional slat (for which the BAF (Slat) method was developed) and a Krueger flap, Yueping Guo has recommended an estimated uniform 1.5 dB reduction in the BAF (Slat) predicted spectral level. A new method for Krueger flap noise prediction from first principles is needed (Ref 36) and could be used in future iterations of this study. The trailing edge noise source is predicted with the FNKAFM (Refs 37, 38) model.

#### **E. Landing Gear and Flap Side Edge Noise Reduction**

ITD50A has developed noise reduction technology for the main landing gear and the flap side-edge airframe components. For the main landing gear, a partial main gear fairing was designed that covers several of the structural elements of the gear and includes porous areas to provide some flow through the fairing and edge serrations to minimize shedding from the sides of the fairing. Of several flap side edge noise reduction components investigated, a porous side edge treatment was considered the most applicable for the N+2 timeframe and is considered applicable across the T+W, OWN, and MFN aircraft. The noise reduction from these two airframe technologies has been verified by ITD50A on the 18% scale model of the G550 (Refs 39, 40) and subsequently analyzed in full-scale, full-fidelity high resolution computations of the noise reduction concepts installed on the G550 geometry (Refs 41, 42). The computed spectral level noise reduction for the partial landing gear fairing is the difference between the unaltered G550 landing gear noise (on a full aircraft geometry) and the landing gear noise (on a full aircraft geometry) with the partial landing gear fairing installed. Similarly for the flap side edge treatment a noise reduction map is provided by ITD50A as a function of polar and azimuthal directivity angles and frequencies.

The noise reduction suppression map for the partial main gear fairing (PMGF) is applied directly in the noise assessment process to the source noise prediction of the main landing gear for all the ERA aircraft. As a function of angle and frequency, the level of noise reduction varies but can be categorized as about a 2 dB level of noise reduction. The impact at the aircraft level will be quantified in the results section.

The noise reduction suppression map for the flap side edge treatment (FSET) is applied directly to the T+W98 Regional Jet aircraft, as it is approximately close in size to the G550 of ITD50A. For all the other T+W, OWN, and MFN aircraft, the level of flap side edge treatment noise reduction is set at a uniform 3 dB over all angles and frequencies. This level is considered to be achievable with this validated technology.

#### **F. Propulsion Airframe Aeroacoustic (PAA) Interaction**

In general, the aeroacoustic effects related to propulsion airframe integration, or PAA effects, can be classified fundamentally as those more associated with flow interaction and those associated with acoustic propagation (Ref 2). With this fundamental division, the classification can be extended further. For flow interaction, the next important division regards the flow direction, upstream or inlet, and downstream or exhaust. Because turbomachinery and jet noise sources have different spectral, spatial distribution and directivity characteristics, acoustic propagation effects are more importantly divided along with noise sources. The classification of PAA from Ref 2 represents a general way of organizing PAA effects, however at the same time, while useful it must be emphasized that these effects cannot necessarily be

studied or addressed separately. Rather the opposite is the case, particularly on a full aircraft configuration in flight as illuminated by Ref 43, which makes the identification and quantification of PAA effects very challenging. Similarly, the development of noise reduction approaches incorporating or taking advantage of PAA effects is necessarily involved with the integrated vehicle design and flight characteristics.

The N+2 aircraft models include the layout of the engines and airframes of the integrated configurations and key dimensions that are a necessary starting point for a prediction of the PAA effects due to acoustic scattering. The integrated design provides the key result of the engine position relative to the airframe, which defines the airframe surface area available to shield or reflect, as appropriate, the inlet radiated engine fan noise and the aft-radiated fan, jet and core noise components. Additional detailed geometry specifications are added as available. For the HWB configuration, ITD51A has developed the engine/airframe integration design using detailed high fidelity computational analysis and wind tunnel testing.

At the conceptual aircraft design stage, the PAA interaction effects from acoustic propagation and scattering are essential to incorporate due to the large impact that shielding and reflection can have for the various conventional and unconventional aircraft configurations. The PAA interaction effects from some flow interactions, such as jet-pylon interaction, can be more difficult to incorporate because high fidelity geometry and computational analysis are generally not available at the conceptual level or within the timeframe required. The PAA effects associated with acoustic scattering can be dependent on details of the configuration platform, the effect of flow velocity on scattering, the aircraft angle of attack, the engine power setting, and the aircraft control surface deflection. Therefore, the challenge in predicting the PAA effects for the many configurations of the ERA portfolio is to prioritize by the impact on system level noise and focus on the acoustic scattering effects of shielding and reflection. Computational prediction of acoustic scattering with high fidelity and mid-fidelity methods has been a developing area over recent years. However, due to the time available, the quantity of configurations to examine, and the variety of flight parameters, it has not been practical to apply computational methods for the current study.

For all the N+2 aircraft, the propulsion airframe aeroacoustics (PAA) acoustic scattering effects are determined with a data-to-prediction process developed from a large database acquired in the first half of ERA. The large database is comprised of PAA experiments including the 14x22 N2A Aeroacoustic Test (Ref 26, 44) and the multiple experiments in the Boeing Low Speed Aeroacoustic Facility (LSAF) (Refs 3, 9, 25, and 45) that include configurations with broadband and jet sources to account for the respective differences in source distribution and directivity characteristics. Following the procedure described in Ref 4, the databases are used to develop noise suppression maps due to acoustic scattering that are a function of configuration, power condition, frequency and both polar and azimuthal directivity angles. Suppression maps are developed for each of the engine noise sources at the correct locations corresponding to the engine inlet plane, core exit plane, and fan nozzle exit plane. Importantly, these databases include the effect on the shielding and reflection from the mean flow and realistic shear layers. Each map is generated by calculating a suppression function for each frequency at every polar,  $\theta$ , and azimuthal,  $\phi$ , angle on the noise source hemisphere. The suppression function,  $S$ , is the ratio of the shielded to unshielded mean square pressures and is given by

$$S(f, \theta, \phi) = \frac{P_{rms}^2(f, \theta, \phi)_{shielded}}{P_{rms}^2(f, \theta, \phi)_{unshielded}} = 10^{\left(\frac{\Delta dB}{10}\right)}$$

where  $\Delta dB = SPL_{shielded} - SPL_{unshielded}$ . Thus  $S < 1$  indicates suppression or reduction and  $S > 1$  indicates amplification or increase. Adjustment to a predicted source noise level and directivity is achieved by applying the appropriate suppression map.

Examples of typical suppression maps for the shielding of broadband noise and the shielding of jet noise by the HWB301 airframe are shown in Figures 4 and 5, respectively. The shielding suppression map of Figure 5 is applied to the fan noise source, at this one frequency, for an engine position where the fan nozzle exit plane is one fan nozzle diameter upstream of the trailing edge along the centerline of the engine. The noise reduction from shielding can be as high as 20 dB; however, it drops rapidly with downstream angles beyond 120 degrees. A different map is applied to shield the core noise source that emanates from the core nozzle exit plane, which is closer to the trailing edge. Figure 5 is the suppression map due to shielding that is applied to the jet source noise, at one frequency. The shielding of jet noise is challenging due to the distributed nature of jet noise (Ref 2). Figure 6 shows the reflection of broadband noise from the T+W301 aircraft, again at one frequency, and is for application to the fan noise source. The reflection

increases noise as much as 4.0 dB at this frequency and with a strong directivity that is the result of the T+W planform. The areas of peak reflected noise are off of the centerline of flight,  $\phi = 0$  degrees, toward azimuthal angles of 45 degrees due to the location of the engines on the wings and due to the dihedral angle of the wings. These maps illustrate the strong directivity generated from propulsion airframe aeroacoustic scattering effects as a result of high fidelity complete aircraft geometry.

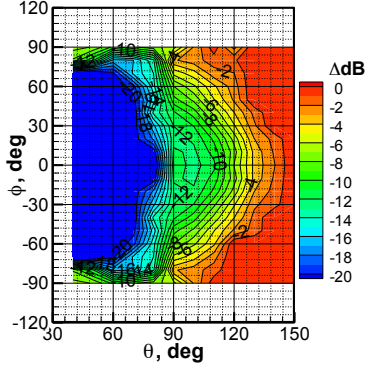


Figure 4. Shielding suppression map for broadband noise at 3150Hz, full-scale, for the HWB301 at approach. Negative  $\Delta$ dB is noise reduction.

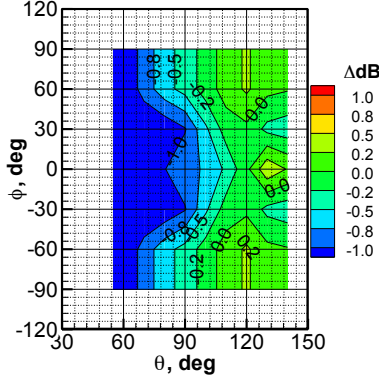


Figure 5. Shielding suppression map for jet noise at 500Hz, full-scale, for the HWB301 at cutback. Negative  $\Delta$ dB is noise reduction, positive is noise increase.

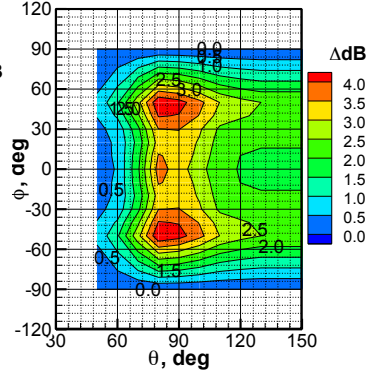


Figure 6. Reflection map for broadband noise at 3150Hz, full-scale, for the T+W301 at cutback. Negative  $\Delta$ dB is noise reduction, positive is noise increase.

### G. Engine and Airframe Noise Source Ranking

A final important aspect of the noise assessment process includes the ranking of the engine and airframe sources to best represent the accurate order of the sources; that is, from highest noise source to lowest in proper order. When computing the aircraft noise of a present day aircraft, the prediction can be calibrated to certification data. Typically, those calibrations are on the order of 1-2 dB for a rigorous prediction at each certification point; however, to achieve this may require larger calibrations on individual engine and airframe component sources. Even with excellent component level predictions, the ranking of sources may not be sufficiently accurate due to many issues. Most likely possibilities are multiple simultaneous effects stemming from some combination of PAA effects, flight effects, and the impacts of full-scale, full-fidelity implementation. For the prediction of advanced, N+2 and unconventional aircraft there is obviously no certification data available to use for calibration. This has presented a unique challenge to the reduction of uncertainty for advanced concept system noise prediction. The initial NASA HWB system noise study (Ref 2) predicted an HWB concept with a GE90-like engine so that the engine source levels and ranking could be calibrated to GE90 information (Ref 46), and for which the uncertainty in the prediction is minimized. As a result, Ref 2 could predict the PAA effects and the total system noise of that HWB concept with greater confidence.

Therefore, for this current study, after the initial prediction of the individual engine and airframe noise sources, an additional adjustment to the ranking of the sources is performed according to the combined experience from Refs 4, 5, 8, 9 and additional information from the ITD51A and ITD35A teams. Based on known airframe source level ranking, both the flap and slat predictions were further adjusted to achieve appropriate noise levels relative to the main landing gear. The adjustment in the core noise level, already discussed in section III.B, is another adjustment to the ranking of sources.

## IV. Results

The system level results for the N+2 portfolio will be discussed first with a focus on the impact of operational characteristics. In the next section, the impact of selected technologies will be highlighted. Finally, an example of the impact that ERA data more relevant to the N+2 design space has on the predictions of ERA data will be shown.

### A. Aircraft System Level Results with a Focus on Operational Characteristics

Figure 7 shows the cumulative system noise of each of the thirteen N+2 vehicles. A second result for each vehicle includes the three additional ITDNR noise reduction (ITDNR) technologies. The first, soft vane, is applied on the stator vanes of all thirteen vehicles. The second, the partial main gear fairing, is applied on all the main gear of the vehicles. And the third, flap side edge treatment, is applied to all vehicles except the HWB vehicles. Of course, the results in Figure 8 are relative to the Stage 4 requirement based on the weight and number of engines for each of the vehicles. The vehicles are grouped by class from smallest class on the left to largest class on the right.

It can be observed that at least one vehicle from each class of vehicles is predicted to have a margin to Stage 4 of at least 40 dB except the smallest class, 98 passengers. This can largely be attributed to the relatively low bypass ratio engines, about ten, on these aircraft. At this small size the integration of higher bypass ratio, larger diameter engines are more challenging.

All the vehicles that are able to reach noise margins of greater than 33 dB to Stage 4 are either the unconventional OWN and MFN or the HWB configurations. This highlights the clear noise advantage of the unconventional configurations to take advantage of PAA noise reduction. The quietest T+W aircraft with engines mounted under the wing is the T+W160 in the single aisle class with a margin of 31.4 dB. It should be noted how remarkable that result is and indicates that even with a conventional engine under the wing installation, very significant noise reduction is still possible in the N+2 timeframe. It is also important to compare this result with a prior NASA study (Ref 29) for an advanced vehicle in this same class. In Ref 29, the single aisle, engine under wing aircraft was assessed at 29 dB cumulative margin to Stage 4. It was considered a noise optimized design with N+1 technology assumptions (N+1 entry-into-service timeframe of 2020) and also included, because of the noise optimized assumption and the information available at the time of the study, much higher assumed levels of noise reduction for airframe (landing gear, slat, and flap side edge) and soft vane technologies.

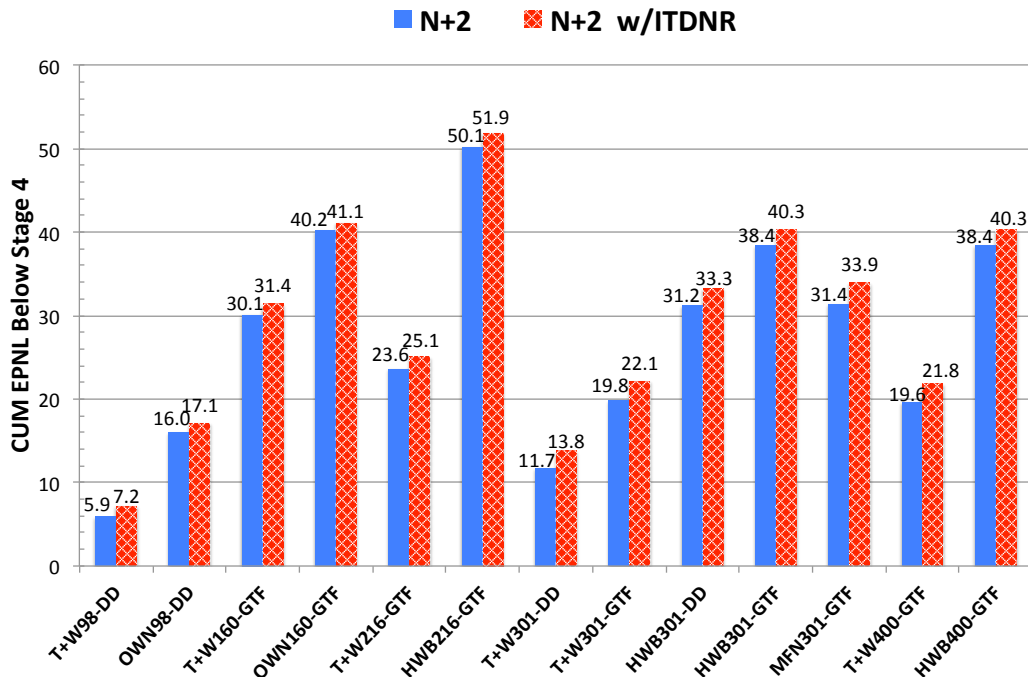


Figure 7. Aircraft system level noise for all ERA N+2 vehicles, relative to the Stage 4 requirement for each vehicle weight. Solid bar is the cumulative noise for the N+2 vehicle, ITDNR (hash bar) adds to each vehicle the impact of three specific technologies: soft vane, partial landing gear fairing and, with the exception of the HWB, flap side edge treatment.



When comparing between configurations it is best to compare within the same class and with the same engine installed on both vehicles. Therefore, the OWN and MFN aircraft should be compared relative to the equivalent T+W aircraft; however, the OWN and MFN cannot be compared directly as they are in different classes and have different engines. Specifically, the OWN160-GTF can be compared directly with the T+W160-GTF showing a 9.7 dB advantage. The MFN301-GTF can be compared with the T+W301-GTF showing the MFN to have an 11.8 dB advantage. It should be noted that one potentially important effect has not been included in either of the OWN aircraft. The nacelles are integrated into the upper surface of the wing introducing an additional jet scrubbing noise source that will likely reduce the margin to Stage 4 and could be included in future updates of this assessment.

Three of the four HWB aircraft have margins over 40 dB with the fourth, HWB301-DD having a margin of 33.3 dB due to the direct drive engine noise differences with the geared engines on the other three. The HWB216 is the standout with a margin of 51.9 dB, an 11.6 dB greater margin compared to the HWB301-GTF. On both aircraft the engines are positioned at the same non-dimensional distance upstream of the trailing edge, the core nozzle exit plane is one fan nozzle diameter upstream of the trailing edge along a line parallel to the engine axis. Tables 3 and 4 show some of the key differences in the engine and airframe parameters. In addition to these differences, much of the 11.6 dB difference can be attributed to operational factors, which will be described now.

Figure 8 plots the altitude and speed of all the T+W, OWN, and MFN aircraft for the takeoff and cutback conditions. Figure 9 plots the altitude and speed for the four HWB aircraft. While speed clusters in the 150 to 180 knot range, the engine and low speed aerodynamic high lift characteristics of each aircraft result in a large range of altitudes for the cutback condition. A 500-foot difference in altitude at cutback, all else equal, can result in a 2.5 dB difference. The differences in speed can impact both noise source levels and the duration effect in the EPNL calculation.

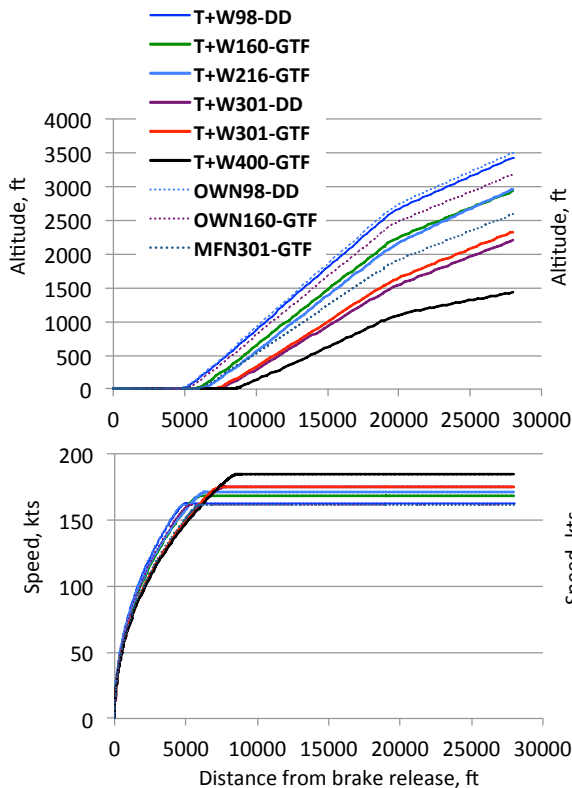


Figure 8. Altitude and speed as a function of distance, takeoff and cutback noise conditions, for all T+W, OWN, and MFN aircraft.

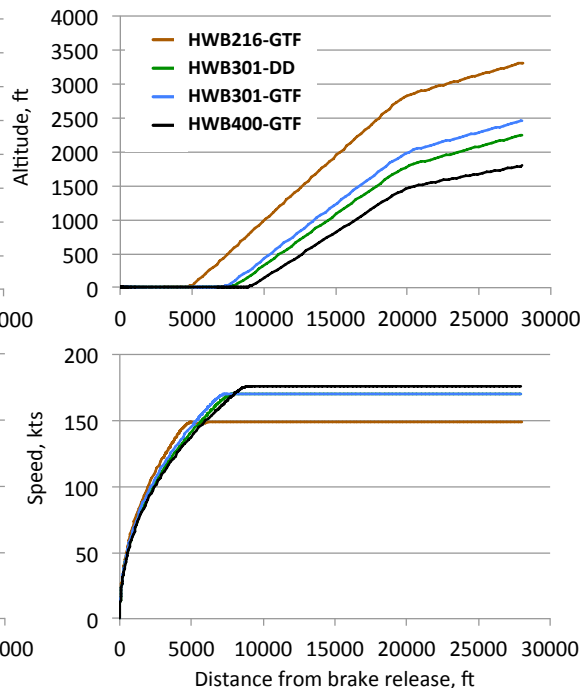


Figure 9. Altitude and speed as a function of distance, takeoff and cutback noise conditions, for all HWB aircraft.

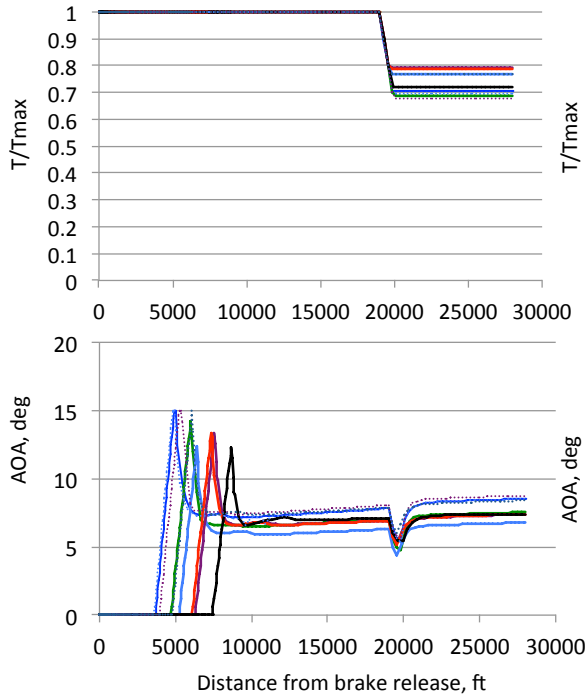


Figure 10. Throttle setting (as a fraction of maximum) and angle of attack as a function of distance, takeoff and cutback points. For all T+W, OWN, and MFN aircraft (same legend as in Figure 8).

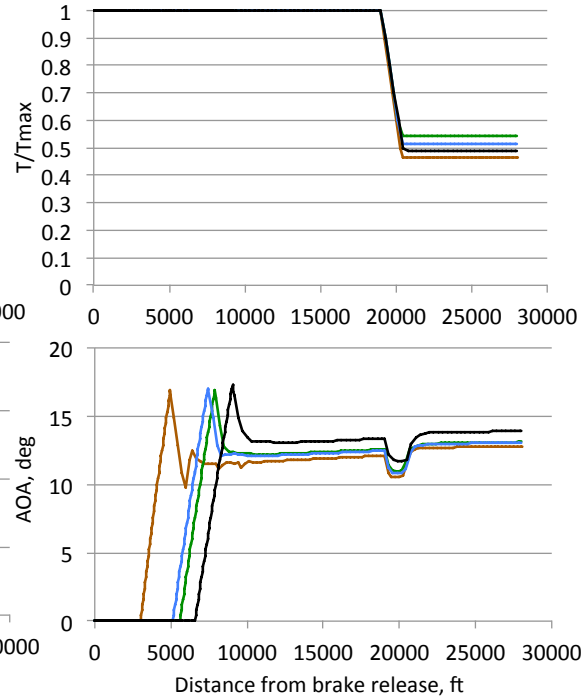


Figure 11. Throttle setting (as a fraction of maximum) and angle of attack as a function of distance, takeoff and cutback points. For all HWB aircraft (same legend as in Figure 9).

Figures 10 and 11 plot the throttle setting and the angle of attack also as a function of distance for takeoff and cutback conditions. Again, the distinct aerodynamic characteristics of the HWB evidence themselves by requiring a much lower throttle setting, around 50% for four HWB aircraft, compared to settings between 70 and 80% for all the T+W, OWN, and MFN aircraft. Also characteristic of the HWB is a higher angle of attack in comparison with the T+W, OWN, and MFN aircraft. The lower throttle setting can lower engine noise at cutback, offset somewhat by the higher angle of attack, which decreases shielding.

Figure 12, for the approach condition, shows the speed, throttle setting and the angle of attack for the T+W, OWN, and MFN aircraft. Figure 13 plots the same quantities for all four HWB aircraft. The HWB aircraft again have lower approach speeds, lower throttle settings, and higher angles of attack.

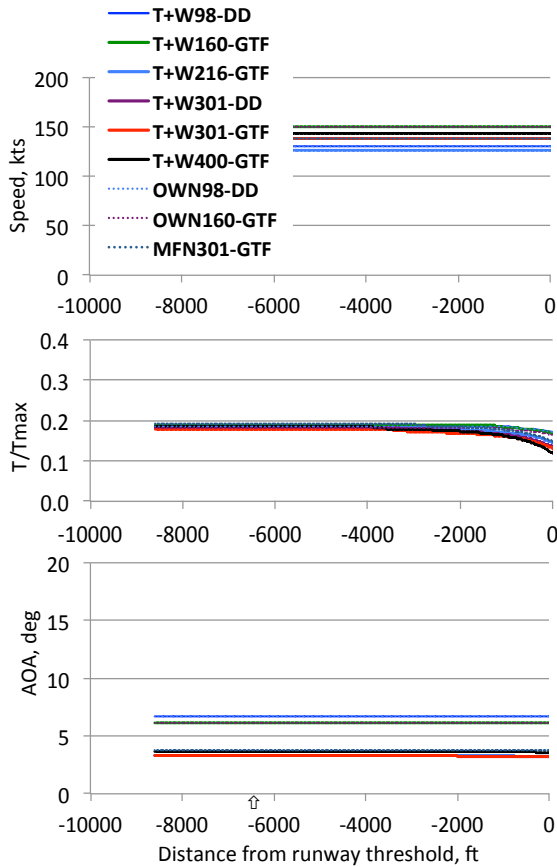


Figure 12. Speed, throttle setting (as a fraction of maximum), and angle of attack for approach condition, all T+W, OWN, and MFN aircraft.

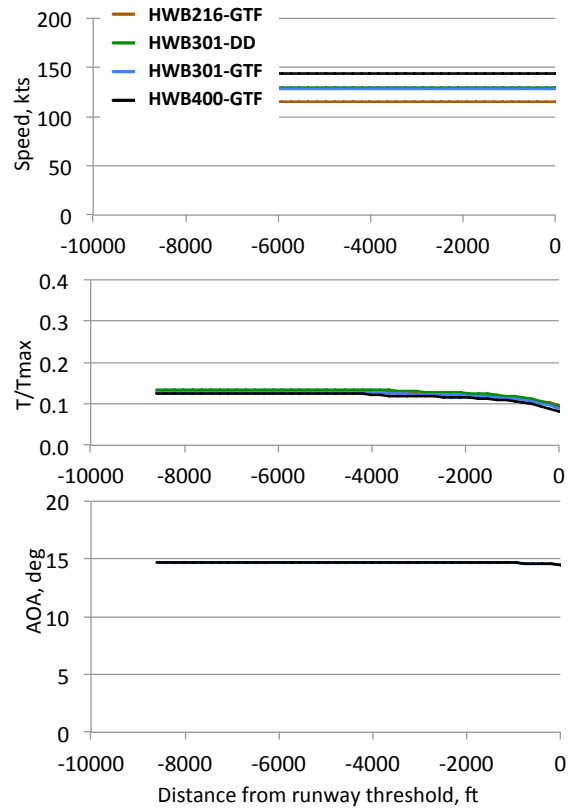


Figure 13. Speed, throttle setting (as a fraction of maximum), and angle of attack for approach condition, all HWB aircraft.

Specifically at the cutback position, the HWB216 as compared to the HWB301 has a higher altitude, a lower throttle setting, a lower speed, and a lower angle of attack. Also, the HWB216 has a lower approach speed. All these operational factors together lower the noise of the HWB216 as compared to the HWB301 by 8 dB and account for the majority of the system level noise difference in margin to Stage 4. As discussed in Ref 6, the HWB216 has a much lower wing loading relative to the other HWB concepts resulting in these operational performance differences, and should be refined in a following design iteration to be more consistent with the other HWB concepts. The remainder of the difference can be accounted with reference to the different class and engines of each aircraft.

Next, a comparison of the T+W301-GTF and the HWB301-GTF is presented in Figures 14 to 17. The comparison uses the tone corrected perceived noise levels (PNLT) of all the predicted noise sources and PAA effects. Figure 14 shows that the T+W at approach condition has the total fan noise (including the effects from duct liner, soft vane and PAA effects from reflection) as the highest source. Figure 15 shows that for the HWB301 at approach, the PAA effects from shielding have greatly reduced the total fan noise source to the point that the main gear followed by the Krueger flap are the first and second highest sources, respectively, with total fan as the third highest source. This is an example of how with a change in configuration, in this case largely from PAA effects, the ranking of the highest sources is altered. Figures 16 and 17 show the comparison between the T+W and the HWB at the sideline condition. In this case, the total fan noise remains the highest source for both configurations. However, the second and third highest sources are changed as a result of the fact that the core noise source is reduced more by shielding as compared to jet noise.

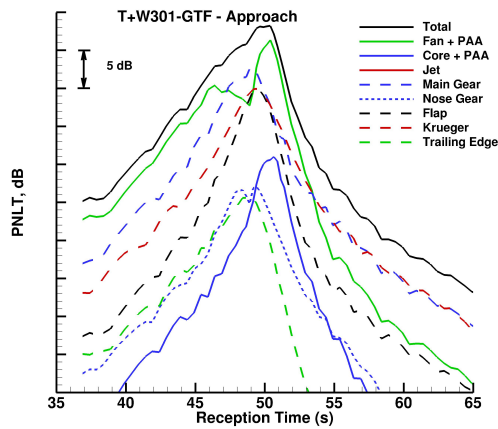


Figure 14. Noise components and total PNLT for the T+W301-GTF, at approach.

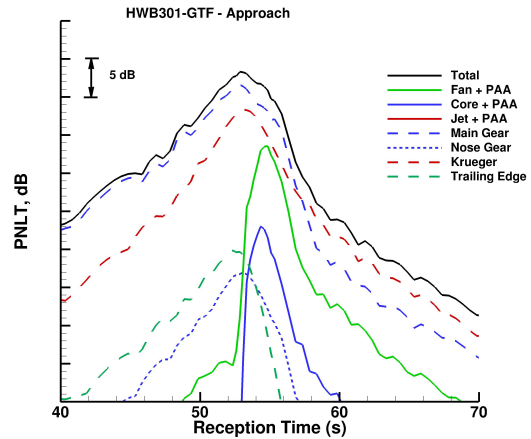


Figure 15. Noise components and total PNLT for the HWB301-GTF, at approach.

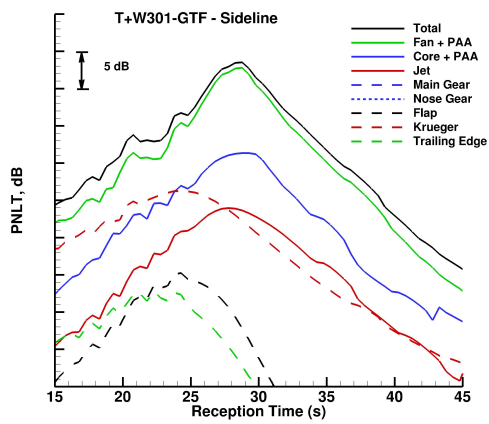


Figure 16. Noise components and total PNLT for the T+W301-GTF, at sideline.

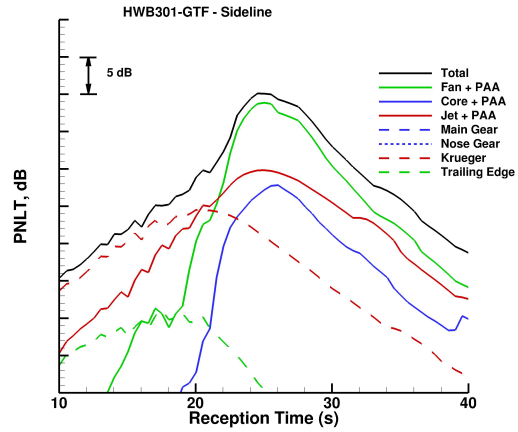


Figure 17. Noise components and total PNLT for the HWB301-GTF, at sideline.

## B. Impact of Selected Technologies

The impact of selected technologies at the aircraft system level can be shown by removing the prediction of the technology from the final assessed level shown in Figure 7. For example, taking the predicted level in Figure 7 and predicting a conventional acoustic liner from the TREAT method in place of the MDOF duct liner can calculate the impact at the aircraft level of the MDOF acoustic liner. For a given aircraft, this would be the impact of the MDOF technology. This can be done, one at a time or “one-off”, for several technologies to give insight into the impact of technologies as influenced by the source ranking. Figure 18 shows the impact of this “one-off” analysis for the HWB301-GTF aircraft that has a system level margin of 40.3 EPNLdB in Figure 7. The PAA technology represents the total shielding noise reduction predicted from shielding the fan, core, and jet noise sources by the HWB airframe. Engine noise is shielded at each of the certification points with a total for all three summing to 7.1 dB cumulative. The impact of the soft vane (SV), MDOF duct liner, partial main gear fairing, and flap side edge treatment are also shown in Figure 18. The soft vane and MDOF liners have the largest impact at sideline and the main gear fairing has an impact at approach. Figure 19 shows the impact of these same technologies on four aircraft from a cumulative perspective.

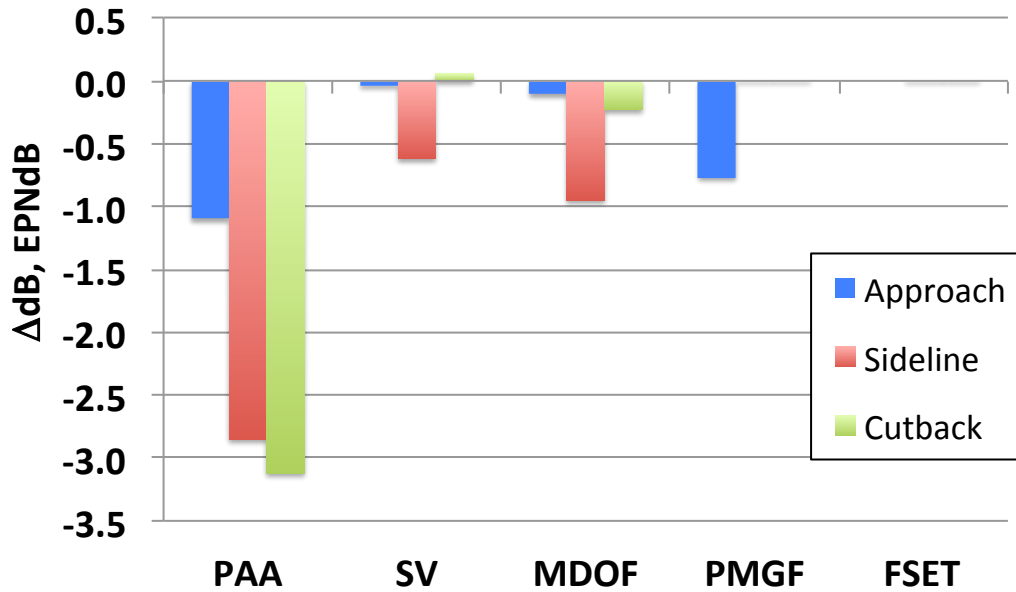


Figure 18. Impact of selected technologies on the aircraft system noise of the HWB301-GTF for each certification point. PAA accounts for shielding and reflection effects, SV is the soft vane, MDOF acoustic duct liner, PMGF is the partial main gear fairing and, FSET is the flap side edge treatment and is not applicable to a HWB. Negative ΔdB is noise reduction.

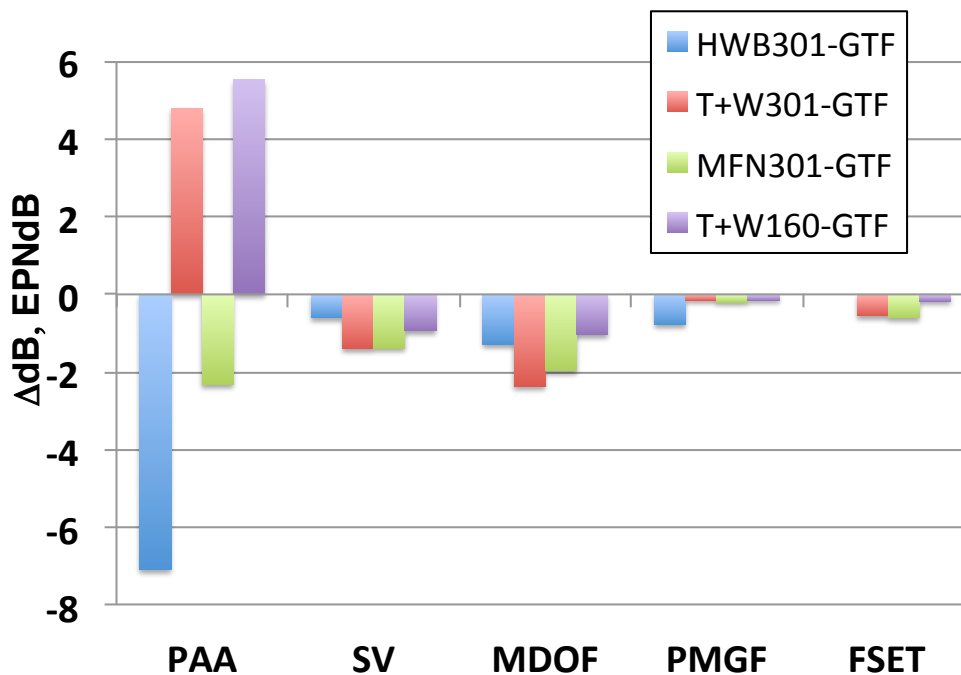


Figure 19. Impact of selected technologies on the cumulative noise of four aircraft. PAA accounts for all shielding and/or reflection, SV is the soft vane, MDOF is the acoustic duct liner, PMGF is the partial main gear fairing, and FSET is the flap side edge treatment. Negative ΔdB is noise reduction.

The total impact of PAA between an HWB and an equivalent T+W can be seen in Figure 19. The HWB301-GTF has a total PAA noise reduction of 7.1 dB while the T+W301-GTF has a total cumulative noise increase from reflection of 4.8 dB. Therefore, the total noise reduction from PAA in changing from a T+W to the HWB configuration is actually 11.9 dB cumulative. Of the other technologies, soft vane and MDOF have the next largest contributions to system noise reduction and also impact all the configurations. The main gear fairing has a larger contribution on the HWB due to ranking as compared to that on the T+W configurations.

### C. Impact of Improved Data and Prediction Methods

Most semi-empirical noise prediction methods, including many of those in ANOPP, contain excellent physical understanding and are functionally robust and well understood. However, in general they are validated by a set of experiments and, therefore, may be limited in applicability by that validation. The ERA N+2 design space is generally outside of the experience base of, at least, some key semi-empirical methods that were already part of ANOPP. An example of the value of the ERA experimental database generated and used in this noise assessment is given in this section for the fan source noise. The HWB301-GTF cumulative system noise is reported at 40.3 EPNLdB in Figure 7. As described in section III.A the fan source noise is predicted with a data-to-prediction process based on experimental results from ITD35A. Without this data, the best available fan noise prediction method would be the Kresja model (Ref 21) already in ANOPP. The Kresja model was used to predict the fan noise of the N+2 engine of the HWB301-GTF, with all other predictions for the HWB301-GTF being the same. This result compared to the result in Figure 7 will reflect the impact of acquiring new data that is more in the relevant N+2 design space, in this case of the low pressure ratio fan of a geared ultra high bypass ratio engine. The results of this exercise are shown in Table 6 below. At the total aircraft cumulative level, the difference is 4.4 dB, again due only to the different fan component noise prediction methods. At each of the certification points, however, the difference is even more apparent with the Kresja model predicting fan component noise 9.4 dB quieter at approach but 4.4 dB louder at cutback and 4.0 dB louder at sideline as compared to the fan noise prediction based on the new data from the ITD35A experiment. This demonstrates the critical need to continue improvement and validation of component prediction capabilities for system noise assessments.

**Table 6. HWB301-GTF total aircraft system noise and fan component noise predicted from experimental fan noise data and from existing Kresja fan noise prediction method.**

	HWB301-GTF From Figure 7 (fan noise predicted from ITD35A data)	HWB301-GTF (fan noise predicted from Kresja fan noise model already in ANOPP)
Total aircraft, cumulative noise below Stage 4	40.3	35.9
Approach – Fan noise component, EPNL dB, relative to prediction used in Figure 7	-	- 9.4
Cutback – Fan noise component, EPNL dB, relative to prediction used in Figure 7	-	+ 4.4
Sideline – Fan noise component, EPNL dB, relative to prediction used in Figure 7	-	+ 4.0

## V. Conclusions

As a result of a three-year multi-disciplinary effort a comprehensive noise assessment has been accomplished for thirteen NASA modeled advanced aircraft concepts. The thirteen vehicles were designed for entry-into-service in the 2025 timeframe and include a complete range of technology assumptions for advanced engine, airframe structures, and high lift systems.

The noise assessment used a combination of the best system noise prediction methods and the best available experimental data produced in recent years, as well as additional information from industry partners. The result is a detailed and rigorous noise assessment for the certification noise of the N+2 aircraft concepts with much greater fidelity than is typical for conceptual level aircraft. The greater fidelity comes from not only knowledge gained throughout the ERA project, but also the extensive use of experimental data directly in the noise prediction process and validation of trends and levels.

For the NASA N+2 aircraft which are designed in a balanced approach to achieve simultaneously the fuel burn, emissions, and noise reduction goals, the results of the noise assessment show that several of the thirteen aircraft approach levels close to or even exceed the NASA goal of 42 dB cumulative below Stage 4. The key to achieving the 42 dB noise goal is an unconventional configuration that installs the engine over the wing or body in order to maximize the propulsion airframe aeroacoustic interaction effects. The HWB configuration that is able to shield both forward and aft-radiated engine noise has the highest levels of noise reduction from shielding. An analysis of the HWB compared to the equivalent engine-under-wing aircraft shows that the low noise levels achieved by the HWB can be attributed to:

- noise reduction from shielding of both forward and aft radiated engine noise (compared to the noise increase from reflection from the engine-under-wing T+W),
- superior low speed aerodynamic performance which results in higher climb performance and altitude at the cutback point and enables lower approach speeds, and
- the absence of a trailing edge high lift flap system noise source.

The HWB and other aircraft are likely to achieve even lower noise levels with developments in four particularly promising areas:

- fan noise shielding effectiveness technology (greater noise reduction from the same airframe shield dimensions),
- Krueger flap noise reduction,
- main landing gear noise reduction, and
- acoustic liner technology for the aft duct and the bifurcators.

This noise assessment of advanced aircraft has highlighted several areas that would be important to improve the confidence of future predictions including:

- aircraft design to include detailed airframe geometry parameters that are important for the prediction of key airframe noise sources and of propulsion airframe aeroacoustic interactions,
- improved fan source noise prediction method for ultra high bypass ratio fans,
- improved core noise prediction method,
- validated methods for proper ranking of engine and airframe sources over a wide range of design parameters and aircraft configurations,
- high fidelity experimental research of the Krueger flap leading edge,
- high fidelity experimental research of the propulsion airframe aeroacoustic interaction of ultra high bypass ratio fan noise from a turbine power fan noise simulator, and
- prediction methods for the propulsion airframe aeroacoustic scattering interactions (shielding and reflection) that can include the details of flow effects, planform and nacelle geometry, and control surface deflections within the system noise cycle time.

### **Acknowledgments**

This aircraft system noise assessment for the ERA N+2 portfolio of advanced technology concepts has been a significant undertaking over a multi-year period. The authors gratefully acknowledge that this high fidelity assessment of conceptual level aircraft has benefited greatly from the contributions of many. Therefore, the authors would like to thank the ERA ITD leads and industry partners, the entire ERA System Analysis team, and a particular thanks to ERA project manager, Fay Collier, for his vision and leadership throughout the six years of ERA. Both Boeing and Pratt & Whitney are thanked for particularly helpful technical discussions. A special thank you to John Rawls and Stuart Pope of the Aeroacoustics Branch for contributions throughout the calculations for this study and for the implementation of many improvements to the ERA noise assessment process. Yueping Guo has contributed valuable expertise on airframe system noise topics. The authors would also like to give a special acknowledgment and thanks to Jeffrey Berton for many consultations on engine system noise topics. The authors also give a special acknowledgment and thanks to Edmane Envia for contributing expertise on the fan source noise prediction process, providing the soft vane noise reduction data, and for developing the improved rotor-stator spacing effect method. Mike Jones and Doug Nark are thanked for their expertise in all aspects of acoustic liners and in particular on MDOF liners and soft vane technology.

## References

1. Hill, G.A., and Thomas, R.H., "Challenges and Opportunities for Noise Reduction Through Advanced Aircraft Propulsion Airframe Integration and Configurations," presented at the 8<sup>th</sup> CEAS Workshop on Aeroacoustics of New Aircraft and Engine Configurations, Budapest, Hungary, Nov. 11-12, 2004.
2. Thomas, R.H., Burley, C.L., and Olson, E.D., "Hybrid Wing Body Aircraft System Noise Assessment with Propulsion Airframe Aeroacoustic Experiments," *International Journal of Aeroacoustics*, Vol. 11 (3+4), pp. 369-410, 2012.
3. Czech, M.J., Thomas, R.H., and Elkoby, R., "Propulsion Airframe Aeroacoustic Integration Effects of a Hybrid Wing Body Aircraft Configuration," *International Journal of Aeroacoustics*, Vol. 11 (3+4), pp. 335-368, 2012.
4. Burley, C.L., Brooks, T.F., Hutcheson, F.V., Doty, M.J., Lopes, L.V., Nickol, C.L., Vicroy, D.D., and Pope, D.S., "Noise Scaling and Community Noise Metrics for the Hybrid Wing Body Aircraft," AIAA Paper 2014-2626.
5. Guo, Y.P., Burley, C.L., and Thomas, R.H., "On Noise Assessment for Blended Wing Body Aircraft," AIAA Paper 2014-365.
6. Nickol, C.L. and Haller, W.J., "Assessment of the Performance Potential of Advanced Subsonic Transport Concepts for NASA's Environmentally Responsible Aviation Project," AIAA SciTech 2016, San Diego, CA, January, 2016, (accepted for publication).
7. Hahn, A.S., "Application of Cart3D to Complex Propulsion-Airframe Integration with Vehicle Sketch Pad," AIAA 2012-0547.
8. Bonet, J.T., Schellenger, H.G., Rawdon, B.K., Elmer, K.R., Wakayama, S.R., Brown, D., and Guo, Y.P., "Environmentally Responsible Aviation (ERA) Project – N+2 Advanced Vehicle Concepts Study and Conceptual Design of Subscale Test Vehicle (STV)," NASA Contract Report 2013-216519, 2013.
9. Guo, Y.P., Nickol, C.L., and Thomas, R.H., "Noise and Fuel Burn Reduction Potential of an Innovative Subsonic Transport Configuration," AIAA Paper 2014-257.
10. Liebeck, R.H., "Design of the Blended-Wing-Body Subsonic Transport," AIAA Paper 2002-0002.
11. Nickol, C.L. and McCullers, L., "Hybrid Wing Body Configuration System Studies," AIAA Paper 2009-931.
12. Guo, Y.P., Brusniak, L., Czech, M.J., and Thomas, R.H., "Hybrid Wing-Body Aircraft Slat Noise," *AIAA Journal*, 1-11, 10.2514/1.J052540, posted online 11 October 2013.
13. Vicroy, D.D., "Blended-Wing-Body Low-Speed Flight Dynamics: Summary of Ground Tests and Sample Results," AIAA Paper 2009-933.
14. Carter, M.B., Vicroy, D.D., and Patel, D., "Blended-Wing-Body Transonic Aerodynamics: Summary of Ground Tests and Sample Results," AIAA Paper 2009-935.
15. Gatlin, G.M., Vicroy, D.D., and Carter, M.B., "Experimental Investigation of the Low-Speed Aerodynamic Characteristics of a 5.8-Percent Scale Hybrid Wing Body Configuration," AIAA Paper 2012-2669.
16. Flamm, J.D., James, K.D., and Bonet, J.T., "Overview of ERA Integrated Technology Demonstration (ITD) 51A Ultra-High Bypass (UHB) Integration for Hybrid Wing Body (HWB)," AIAA SciTech 2016, San Diego, CA, (accepted for publication).
17. Lytle, J.K., "Numerical Propulsion System Simulation: An Overview," NASA TM 209915, 2000.
18. Tong, M.T., and Naylor, B.A., "An Object-Oriented Computer Code for Aircraft Engine Weight Estimation," GT2008-50062, ASME Turbo-Expo June, 2008.
19. Lopes, L.V., and Burley, C.L., "Design of the Next Generation Aircraft Noise Prediction Program: ANOPP2," AIAA Paper 2011-2854.
20. Van Zante, D.E. and Suder, K.L., "Environmentally Responsible Aviation: Propulsion Research to Enable Fuel Burn, Noise and Emissions Reduction," ISABE-2015-20209, October, 2015.
21. Kresja, E.A. and Stone, J.R., "Enhanced Fan Noise Modeling for Turbofan Engines," NASA/CR-2014-218421, December, 2014.
22. Dahl, M.D., editor, "Assessment of NASA's Aircraft Noise Prediction Capability," NASA TP-2012-215653, July 2012.
23. Emmerling, J. J., Kazin, S. B., and Matta, R. K., "Core Engine Noise Control Program. Volume III, Supplement 1 - Prediction Methods," FAA-RD-74-125, III-I, Mar. 1976. (Available from DTIC as AD A030 376).
24. Stone, J.R., Kresja, E.A., Clark, B.K., and Berton, J.J., "Jet Noise Modeling for Suppressed and Unsuppressed Aircraft in Simulated Flight," NASA/TM-2009-215524, March 2009.
25. Thomas, R.H., Czech, M.J., and Doty, M.J., "High Bypass Ratio Jet Noise Reduction and Installation Effects Including Shielding Effectiveness," AIAA 2013-541.
26. Doty, M.J., Brooks, T.F., Burley, C.L., Bahr, C.J., and Pope, D.S., "Jet Noise Shielding Provided by a Hybrid Wing Body Aircraft," AIAA 2014-2625.
27. Mead, C. and Kenning, O., "Noise and Flow Studies of Coaxial Jets at Incidence," AIAA Paper 2003-3213.
28. Kontos, K.B., Kraft, R.E., and Gliebe, P.R., "Improved NASA-ANOPP Noise Prediction Computer Code for Advanced Subsonic Propulsion Systems, Volume 2: Fan Suppression Model Development," NASA CR-202309, December, 1996.
29. Berton, J.J., Envia, E., and Burley, C.L., "An Analytical Assessment of NASA's N+1 Subsonic Fixed Wing Project Noise Goal," AIAA 2009-3144.
30. Jones, M.G., Parrott, T.L., Sutliff, D.L., and Hughes, C.E., "Assessment of Soft Vane and Metal Foam Engine Noise Reduction Concepts," AIAA 2009-3142.



31. Jones, M.G., Howerton, B.M., and Ayle, E., "Evaluation of Parallel-Element, Variable-Impedance, Broadband Acoustic Liner Concepts," AIAA Paper 2012-2194.
32. Guo, Y.P., "An Improved Landing Gear Noise Prediction Scheme," NASA/CR NAS1-NNL04AA11B Task NNL06AB63T, The Boeing Company, Huntington Beach, CA, November 2006.
33. Guo, Y.P., Burley, C.L., and Thomas, R.H., "Landing Gear Noise Prediction and Analysis for Tube-and-Wing and Hybrid Wing Body Aircraft," AIAA SciTech 2016, San Diego, CA, January, 2016, (accepted for publication).
34. Guo, Y., "Empirical Prediction of Aircraft Flap Side Edge Noise," NASA/CR NAS1-00086 Task NNL04-AD34T, The Boeing Company, Huntington Beach, CA, August 2005.
35. Sen, R., Hardy, B., Yamamoto, K., Guo, Y., and Miller, G., "Airframe Noise Sub-component Definition and Model," Boeing Commercial Airplane Company, NASA/CR-2004-213255, September 2004.
36. Guo, Y.P., Burley, C.L., and Thomas, R.H., "Modeling and Prediction of Krueger Device Noise," abstract submitted to the 22<sup>nd</sup> CEAS/AIAA Aeroacoustics Conference, May, 2016.
37. Fink, M., "Airframe Noise Prediction Method," FAA-RD 77-29, U.S. Department of Transportation, Federal Aviation Administration, 1977.
38. Fink, M., "Noise Component Method for Airframe Noise," *AIAA Journal of Aircraft*, Vol. 16, No. 10, 1979, pp. 659-665.
39. Khorrami, M.R., Humphreys, W.M., Lockard, D.P., and Ravetta, P.A., "Aeroacoustic Evaluation of Flap and Landing Gear Noise Reduction Concepts," AIAA Paper 2014-2478.
40. Khorrami, M.R., Humphreys, W.M., and Lockard, D.P., "An Assessment of Flap and Main Landing Gear Noise Abatement Concepts," AIAA Paper 2015-2987.
41. Khorrami, M.R. and Mineck, R.E., "Toward Full Aircraft Noise Prediction: Detached Eddy Simulations," AIAA Paper 2014-2480.
42. Fares, E., Casalino, D., and Khorrami, M.R., "Evaluation of Airframe Noise Reduction Concepts via Simulations using a Lattice Boltzmann Approach," AIAA Paper 2015-2988.
43. Elkoby, R., "Full-Scale Propulsion Airframe Aeroacoustics Investigation," AIAA Paper 2005-2807.
44. Hutcheson, F.V., Brooks, T.F., Burley, C.L., Bahr, C.J., Stead, D.J., and Pope, D.S., "Shielding of Turbomachinery Broadband Noise by a Hybrid Wing Body Aircraft Configuration," AIAA Paper 2014-2624.
45. Czech, M.J. and Thomas, R.H., "Open Rotor Aeroacoustic Installation Effects for Conventional and Unconventional Airframes," AIAA Paper 2013-2185.
46. Gliebe, P.R., "The GE90: Quiet by Design- Quieter Aircraft Engines Through Leveraging New Technologies," Presentation for 2003 Berkeley Airport Noise Symposium Doing the Wright Stuff: 100 years of Aviation and the Environment, <http://www.its.berkeley.edu/techtransfer/events/air/2003/pdf/gliebe03.pdf>, March 11, 2003.